

## An Anatomical Investigation Regarding the Parietal Foramen in 174 Adult Parietal Bones

Latif Sağlam,<sup>1</sup> İrşad Allahverdiyev,<sup>2</sup> Ali Efruz Sordi,<sup>2</sup> Adnan Öztürk<sup>3</sup>

<sup>1</sup>Department of Anatomy, İstanbul University, İstanbul Faculty of Medicine, İstanbul, Türkiye

<sup>2</sup>İstanbul University, İstanbul Faculty of Medicine, İstanbul, Türkiye

<sup>3</sup>Department of Anatomy, İstanbul Health and Technology University Faculty of Medicine, İstanbul, Türkiye



This study was presented in the 27<sup>th</sup> International Medical Sciences Student Congress, İstanbul, Türkiye, May 14–15, 2022.

This study has also been published as a preprint form and the link is below:  
<http://bit.ly/3Wq9jMS>

### Cite this article as:

Sağlam L, Allahverdiyev İ, Sordi AE, Öztürk A. An Anatomical Investigation Regarding the Parietal Foramen in 174 Adult Parietal Bones. J Clin Pract Res 2025;47(1):60–67.

### Address for correspondence:

Latif Sağlam.  
Department of Anatomy,  
İstanbul University Faculty of  
Medicine, İstanbul, Türkiye  
**Phone:** +90 212 414 20 00  
**E-mail:**  
latif.saglam@istanbul.edu.tr

**Submitted:** 14.08.2024

**Revised:** 26.09.2024

**Accepted:** 09.01.2025

**Available Online:** 03.02.2025

Erciyes University Faculty of  
Medicine Publications -  
Available online at [www.jcpres.com](http://www.jcpres.com)



This work is licensed under  
a Creative Commons  
Attribution-NonCommercial  
4.0 International License.

### ABSTRACT

**Objective:** Investigating all anatomical aspects of the parietal foramen (PF) is essential. This study aimed to examine the anatomical features of the PF.

**Materials and Methods:** A total of 174 dry adult human parietal bones (81 right and 93 left) were carefully examined. The frequency, shape, and direction of the PF were recorded. Measurements included the diameter of the PF (DPF), the distance of the PF to the sagittal suture (DSS), the distance of the PF to the occipital angle (DPO), and the length of the sagittal suture (LSS). Additionally, to determine the topography of the PF (TPF), the LSS/DPO ratio was calculated. The DPF was measured using needles of various diameters, while all distances were measured using a digital caliper.

**Results:** Among the parietal bones, 112 (64.3%) had the PF, while 62 (35.7%) had none. A total of 118 PFs were identified on the 112 bones: 52 on the right side, 58 on the left side, and 8 on the sagittal suture. The foramen was single in 90.7% of cases, double in 6.8%, and triple in 2.5%. The parietal foramen appeared circular in 94.1% and oval in 5.9% of cases. Most foramina were oriented in a posteroanterior direction. The mean measurements for DPF, DSS, DPO, and LSS were  $1.7 \pm 0.6$  mm,  $6.81 \pm 3.40$  mm,  $33.81 \pm 12.43$  mm, and  $108.94 \pm 6.91$  mm, respectively. Additionally, the TPF was approximately 3:1.

**Conclusion:** The data obtained in this study may be important for enhancing the success rate of invasive procedures involving the PF or its adjacent structures, as well as for reducing or preventing complications.

**Keywords:** Parietal foramen, sagittal suture, distance, topography.

### INTRODUCTION

The parietal foramen (PF) is a small, inconsistent opening that may be located on one or both parietal bones near the sagittal suture, at the posterior aspect of the parietal bone. It is situated approximately 3.5 cm anterior to the lambda.<sup>1</sup> The diameter of the PF usually ranges from 1 to 2 but can reach up to 5 mm.<sup>2</sup> A PF exceeding 5 mm in diameter is considered enlarged.<sup>3</sup>

The valveless parietal emissary vein (PEV) passes through the PF, connecting the extracranial veins (scalp veins) to the superior sagittal sinus (SSS). Additionally, this vein is connected to the diploic vein within the spongy layer of the skull bones.<sup>4</sup> Due to the valveless nature of these veins, blood flow is bidirectional.<sup>5</sup> While this characteristic can be advantageous, it can lead to the spread of infection from the scalp to the dural venous sinuses during injury or surgery.<sup>6–8</sup>

The PF rarely transmits anastomotic arteries connecting the scalp arteries to branches of the middle meningeal arteries, as well as a meningeal branch of the occipital artery.<sup>1,3,5</sup> The PF also functions in regulating intracranial temperature and maintaining intracranial pressure during changes in head position.<sup>6</sup> Since the PF and the PEV passing through it are directly associated with the SSS, it is used as a landmark for identifying the SSS on radiologic imaging.<sup>3</sup> Therefore, all anatomical variations of the PF should be known in detail as they have clinical implications.

The prevalence and location of the PF have been reported to vary among different ethnic groups.<sup>6,8–10</sup> The anatomical variations of the PF are not rare, and it is important to understand these variations in detail across different population groups to facilitate invasive procedures.<sup>11</sup>

Considering the clinical importance of the PF, we aimed to investigate its frequency, shape, direction, diameter, topographic location, and distances to certain landmarks, as well as to assert its possible clinical implications.

## MATERIALS AND METHODS

In this cross-sectional anatomical study, a total of 174 (81 right and 93 left) dry adult human parietal bones with unknown age, gender, and race were examined in the Department of Anatomy, İstanbul Faculty of Medicine, İstanbul University. These samples were collected between 1980 and 2020. None of the bones had any deformity or damage. The present study was approved by the Clinical Research Ethical Committee of İstanbul University, İstanbul Faculty of Medicine (IRB-Institutional Review Board; number: 2022/462). All samples were carefully examined, and the following parameters were investigated for each parietal bone.

### Morphological Parameters

- The number and shape of the PFs were macroscopically inspected on each bone and noted.
- A needle with a diameter of 0.5 x 80 mm was used to define the patency and direction of the PF (Fig. 1). Any foramen smaller than the needle's diameter was excluded from the analysis and not reported.

## KEY MESSAGES

- A total of 174 dry adult human parietal bones were examined.
- The frequency, shape, and direction of the parietal foramen (PF) were investigated. Additionally, the diameter of PF, distance of PF to the sagittal suture, distance of PF to the occipital angle, length of the sagittal suture, and the topographical location of PF were measured.
- This study provides more anatomical details than previous ones conducted in Türkiye.

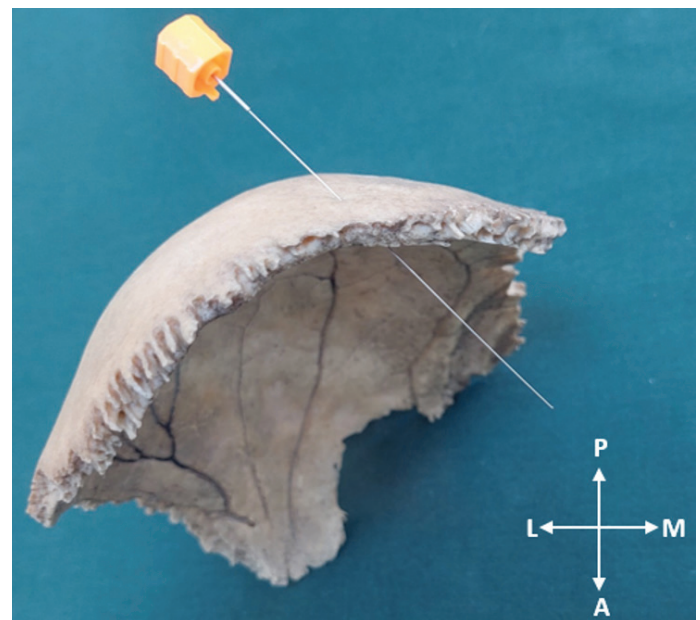


**Figure 1.** Determination of the patency, direction, and diameter of the parietal foramen using a needle.

A: Anterior; P: Posterior; L: Lateral; M: Medial.

### Morphometric Parameters

- Diameter of the Parietal Foramen (DPF): Needles with different diameters (0.5 mm, 0.8 mm, 1.0 mm, 1.25 mm, etc.) were used, and the obtained data were recorded.
- Distance of the PF to the Sagittal Suture (DSS): The shortest distance between the PF and the sagittal suture was measured (Fig. 2). If the foramen was located on the sagittal suture, the DSS was recorded as 0.
- Distance of the PF to the Occipital Angle (DPO): The distance from the PF to the transverse line passing over the tip of the occipital angle was measured (Fig. 2).

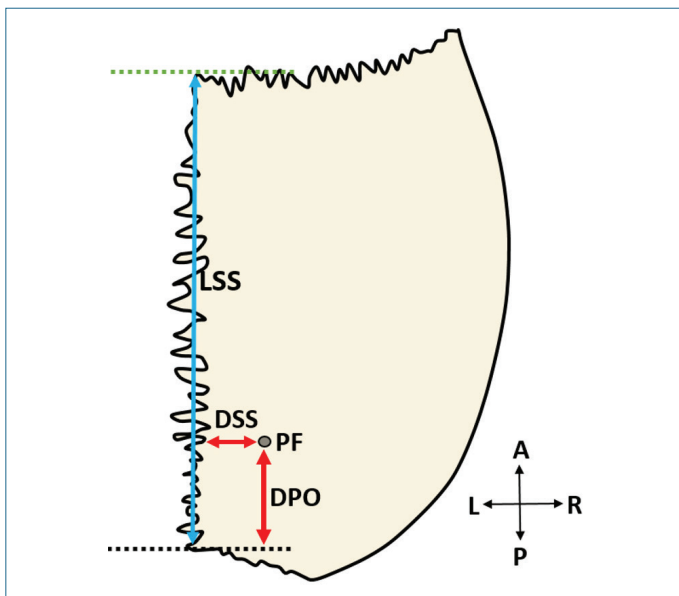


**Figure 2.** Representation of the distances from the parietal foramen to specific landmarks, superior view, right. PF: Parietal Foramen; LSS (vertical bidirectional blue arrow): Length of the Sagittal Suture; DSS (transverse bidirectional red arrow): Distance of the PF to the Sagittal Suture; DPO (vertical bidirectional red arrow): Distance of the PF to Occipital Angle. The dotted green line demonstrates the transverse line passing over the tip of the frontal angle, and the dotted black line indicates the transverse line passing over the tip of the occipital angle.

A: Anterior; P: Posterior; L: Left; R: Right.

- Length of the Sagittal Suture (LSS): The distance between the tip of the frontal and the occipital angle was defined as the LSS (Fig. 2).
- Topography of the PF (TPF): To determine the topography, the LSS/DPO ratio was calculated.

The distances related to the PF were measured using a digital caliper accurate to 0.01 mm (INSIZE Co., Ltd., Taiwan). Two independent and experienced researchers (L.S. and A.O.) performed all measurements.

### Statistical Analysis

The IBM SPSS (Statistical Package for the Social Sciences) version 21.0 was used to evaluate and analyze the data. Since the gender of the parietal bones was unknown and it was unclear whether the bone samples belonged to the same individual, comparisons of these bone measurements in terms of gender and side could not be made. The Shapiro-Wilk test was used to assess the distribution of variables. For

the variables in the measurements, descriptive statistics (e.g., mean and standard deviation) were used. Continuous variables were presented as median (minimum: maximum) and mean  $\pm$  standard deviation values. Frequency (n) and percentage (%) values were used for categorical variables.

To evaluate the reliability of the measurements, the technical error of measurement (TEM), relative technical error of measurement (rTEM), and coefficient of reliability (R) were calculated.

The TEM provides a standard deviation-like measure of the magnitude of error and is expressed as the typical error magnitude associated with a particular measurement. This value can be used to assess both intra-observer reliability and inter-observer agreement. The main difference from the standard deviation value is that both measurement (inter-observer) values are calculated.<sup>12,13</sup>

The rTEM represents an estimate of error magnitude relative to the size of the measurement and is expressed as a percentage (%). It is calculated by dividing the TEM for a given variable by the mean of that variable and multiplying the result by 100.<sup>12-14</sup>

The R represents the proportion of between-subject variance free from measurement error. It ranges between 0 (not reliable) and 1 (completely reliable). This value can be calculated using the formula  $R = 1 - [(TEM)^2 / (SD)^2]$ . In this formula, "SD" refers to the standard deviation of the first and second measurements.<sup>12,13,15</sup>

## RESULTS

We observed that 112 (64.3%) of the parietal bones had a PF, while 62 (35.7%) did not (Fig. 3a). A total of 118 PFs were detected on these 112 bones: 52 on the right side, 58 on the left side, and 8 on the sagittal suture (SS) (Fig. 3c-e).

The vast majority of foramina were single (90.7%) (Fig. 3b). Four double PFs (one on the right side and three on the left side) (Fig. 3c) and one triple PF (on the left side) (Fig. 3c) were observed. Similarly, most of the PFs were circular (94.1%) (Fig. 3b), with oval shapes accounting for the remaining 5.9% (Fig. 3c). Many of the foramina were found to be open (70.4%). Additionally, the direction of most of the foramina was posteroanterior. Table 1 summarizes the results related to the morphological features of the PF.

The overall results and the distribution of the morphometric features of the PF in terms of sides are shown in Table 2. The overall DPF, DSS, DPO, and LSS were obtained as means of  $1.7 \pm 0.6$  mm,  $6.81 \pm 3.40$  mm,  $33.81 \pm 12.43$  mm, and  $108.94 \pm 6.91$  mm, respectively. Additionally, the TPF, calculated as the LSS/DPO ratio, was approximately 3:1. The

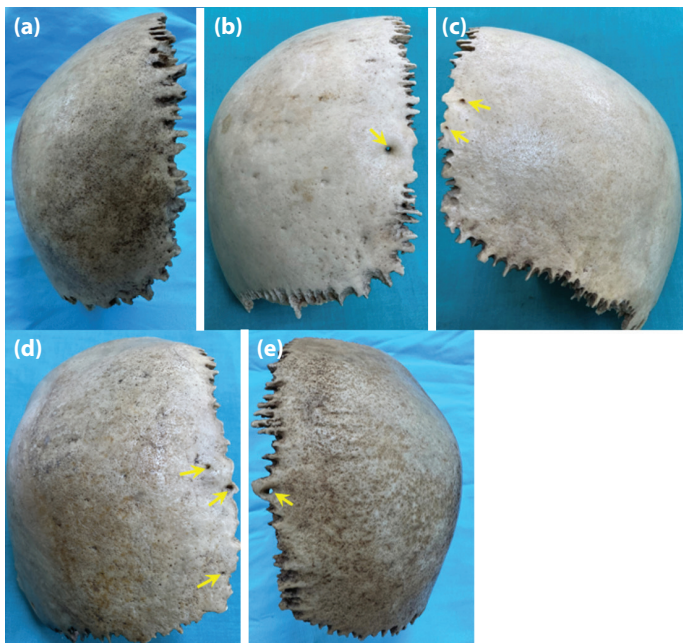


**Figure 3.** Demonstration of the anatomical features of the parietal foramen. **(a)** Absent parietal foramen, left; **(b)** Single and circular parietal foramen, left; **(c)** Double and oval parietal foramen, right; **(d)** Triple parietal foramen, left; **(e)** Parietal foramen on the sagittal suture. The yellow arrows point to the parietal foramen.

reliability analysis of the morphometric data is presented in Table 3. Smaller TEM values, indicating higher precision, affirm the reliability of the measurements, with values ranging from 0.24 to 0.70. Similarly, from a reliability perspective, our results are highly satisfactory, as lower rTEM percentages, ranging from 0.66% to 2.88%, indicate more accurate measurements. Lastly, our R values, which are close to the maximum value of 1, further confirm reliability, as higher R values signify greater precision in measurements.

## DISCUSSION

### Morphological Features

No consensus exists among researchers regarding the frequency of the PF, its distribution between sides, and its presence on the SS (Appendix). The prevalence of PF has been reported to be lowest in the United States at 50% and highest in Thailand at 86%.<sup>16,17</sup> Similarly, the frequency of bilateral PF has been reported as lowest in Europe at 24.2% and highest in Türkiye at 74.65%, while the frequency of unilateral PF has been stated as lowest in the United States at 20% and highest in China at 66.07%.<sup>8,10,18</sup> Additionally, the frequency of PF on the SS was recorded as lowest in Japan at 0.7% and highest in Türkiye at 33.7%.<sup>7,18</sup> The frequency

of the PF in our study (64.3%) appears to be very similar to the findings of Keskil et al.,<sup>9</sup> who reported a prevalence of 63% in a study conducted in Türkiye. However, our results are inconsistent with those of a more recent study in Türkiye by Guzelad et al.<sup>18</sup> Since the parietal bones in our study were not bilateral (i.e., they did not belong to the same individuals), we were unable to report bilateral and unilateral frequencies or compare them with previous studies. In our study, the frequency of PF on the SS was calculated as 4.59%, which aligns closely with findings reported by Keskil et al.,<sup>9</sup> Yoshioko et al.,<sup>17</sup> and Naidoo et al.<sup>19</sup>

The presence and number of PF have been reported at different rates in the literature. In a study on 280 dry skulls, Liu et al.<sup>10</sup> stated that all the PFs observed were single. Murlimanju et al.<sup>20</sup> examined a total of 232 bilateral parietal bones and reported that PF was single in 73 parietal bones (62.9%), double in 8 bones (6.9%), and triple in 2 parietal bones (1.7%). Similarly, Gangmei et al.<sup>21</sup> studied 96 parietal bones bilaterally and found that PF was single in 71 bones, double on 2 right sides, and triple on 1 right side. Fating and Pawar<sup>22</sup> examined 400 parietal bones bilaterally and found that PF was single in 113 right bones (56.5%) and 119 left bones (59.5%), double in 4 right bones (2%), and 1 left bone (0.5%). In our study, 112 of a total of 174 bones had PF. Of the 112 parietal bones, 107 (61.4%) had single PF, 4 had double PF (2.29%), and 1 had triple PF (0.5%).

In terms of the shape of the PF, very few studies have documented its features. de Souza Ferreira et al.<sup>6</sup> reported that the vast majority of PFs were round. Mahakkanukrauh et al.<sup>16</sup> observed three different shapes: circular (94%), oval (4%), and irregular (2%). Similarly, Guzelad et al.<sup>18</sup> observed circular, oval, slit-like, and enlarged PFs in their study but did not report the rate of these shapes. In the current study, we observed circular (94.1%) and oval (5.9%) PF types.

In this study, most of the PFs were open (70.4%). Al-Shuaili et al.<sup>5</sup> observed incomplete PF without intracranial communication in 2% (9/440) of cases. There is a significant difference between the results of these two studies, possibly due to differences in sample size.

In their observational study of 560 parietal bones bilaterally, Liu et al.<sup>10</sup> classified 178 bones with single-hole PF according to their directions. They reported the following distribution: 39.70% (46) anteromedial direction, 17.65% (21) anterior direction, 13.24% (15) anterolateral direction, 13.24% (15) anterosuperior direction, 11.76% (14) anteroinferior direction, 2.94 (3) mediosuperior direction, and 1.47% (2) medioinferior direction. In our study, the direction of all PF was investigated. It was observed that 61.9% (73) had a posteroanterior direction,

**Table 1.** Morphological features of the parietal foramen

Parameter	Right side		Left side		On the SS		Total	
	n	%	n	%	n	%	n	%
Types of PF								
Single	50	96.1	49	84.5	8	100	107	90.7
Double	1	3.9	3	10.3	–	–	4	6.8
Triple	0	0	1	5.2	–	–	1	2.5
Total	52	100	58	100	8	100	118	100
Shape of PF								
Circular	51	98.1	55	93.3	5	71.5	111	94.1
Oval	1	1.9	4	6.7	2	28.5	7	5.9
Total	52	100	59	100	7	100	118	100
Patency of PF								
Open	40	76.9	38	64.4	5	71.5	83	70.4
Closed	12	23.1	21	35.6	2	28.5	35	29.6
Total	52	100	59	100	7	100	118	100
Direction of PF								
PA	27	51.9	41	69.4	5	71.4	73	61.9
AP	2	3.8	2	3.4	1	14.3	5	4.3
LM	5	9.6	3	5.1	–	–	8	6.8
ML	–	–	4	6.8	–	–	4	3.4
PA oblique	13	25	6	10.2	1	14.3	20	16.9
AP oblique	1	1.9	1	1.7	–	–	2	1.7
LM oblique	3	5.9	–	–	–	–	3	2.5
ML oblique	1	1.9	2	3.4	–	–	3	2.5
Total	52	100	59	100	7	100	118	100

PF: Parietal foramen; SS: Sagittal suture; PA: Posteroanterior; AP: Anteroposterior; LM: Lateromedial; ML: Mediolateral.

**Table 2.** Morphometric features of the parietal foramen

Parameter	Right side (n=52)	Left side (n=58)	On the SS (n=8)	Total (n=118)
	Mean±SD (mm)	Mean±SD (mm)	Mean±SD (mm)	Mean±SD (mm)
DPF	1.83±0.8	1.6±0.52	1.67±0.64	1.7±0.6
DSS	6.56±3.28	7.05±3.53	–	6.81±3.40
DPO	34.08±13.30	33.79±12.31	32.24±7.53	33.81±12.43
LSS	108.68±6.40	108.51±7.35	113.34±6.31	108.94±6.91
LSS/DPO ratio (TPF)	Approx. 3:1	Approx. 3:1	Approx. 3:1	Approx. 3:1

DPF: diameter of the parietal foramen; DSS: Distance of the parietal foramen to the sagittal suture; DPO: Distance of the parietal foramen to the occipital angle; LSS: Length of the sagittal suture; TPF: Topography of the parietal foramen; SD: Standard deviation.

16.9% (20) a posteroanterior oblique direction, 6.8% (8) a lateromedial direction, 4.3% (5) an anteroposterior direction, 3.4% (4) a mediolateral direction, 2.5% (3) a lateromedial oblique direction, 2.5% (3) a mediolateral oblique direction, and 1.7% (2) an anteroposterior direction. The results of our study and those of Liu et al.<sup>10</sup> are inconsistent. This discrepancy

**Table 3.** Reliability analysis results

Parameter	TEM	rTEM (%)	R
DPF	0.41	1.34	0.99
DSS	0.24	2.88	0.99
DPO	0.58	2.05	0.99
LSS	0.70	0.66	0.99

TEM: Technical error of measurement; rTEM: Relative technical error of measurement; R: Coefficient of reliability; DPF: Diameter of the parietal foramen; DSS: Distance of the parietal foramen to the sagittal suture; DPO: Distance of the parietal foramen to the occipital angle; LSS: Length of the sagittal suture; TPF: Topography of the parietal foramen.

may be explained by the fact that we evaluated the direction of all PFs in our study. Additionally, differences in sample sizes may contribute to this inconsistency.

### Morphometric Features

The reliability analysis results of morphometric data regarding PF indicate that the findings of the study are reliable. A list of diameter measurements from studies reported in the literature is provided in the Appendix.<sup>5–11,16–23</sup> In our study, the overall DPF was  $1.7 \pm 0.6$  mm. These results are consistent with the findings reported by Guzelad et al.,<sup>18</sup> Mann et al.,<sup>7</sup> and van der Walt et al.<sup>8</sup>

The mean DSS in this study was  $6.81 \pm 3.40$  mm. A summary of DSS findings from previous studies is provided in the Appendix. Our results align with those reported by Fating and Pawar<sup>22</sup> and Murlimanju et al.<sup>20</sup>

Collipal et al.<sup>24</sup> determined that the PF was located at the junction of the SS with the lambda. Tsutsumi et al.<sup>3</sup> reported that the localization of PF was on the SSS. Shmarhalov et al.<sup>11</sup> stated that the most common location of PF was at the side of the sagittal suture, midway between the vertex and the lambda. However, Murlimanju et al.,<sup>20</sup> Shantharam and Manjunath,<sup>25</sup> and Halagatti and Sagar<sup>26</sup> reported that PF was located between the middle and posterior one-third of the parietal bones. In this study, the mean LSS and DPO were  $108.94 \pm 6.91$  mm and  $33.81 \pm 12.43$  mm, respectively. The LSS/DPL ratio (topography of the parietal foramen [TPL]) was approximately 3:1. These results are almost the same as those reported by Murlimanju et al.,<sup>20</sup> Shantharam and Manjunath,<sup>25</sup> and Halagatti and Sagar.<sup>26</sup>

### Clinical Relevance

The parietal bone begins to develop from the intramembranous center near the eminence during the 8<sup>th</sup> week of fetal life. This center radiates toward the periphery in a sunburst design.<sup>27,28</sup> The parietal bone, which is almost

square-shaped, joins the frontal bone anteriorly, the temporal and sphenoid bones inferiorly, the occipital bone posteriorly, and the parietal bone contralaterally.<sup>1</sup>

The obelion is named for its resemblance to the Greek symbol obelos (÷). The central dash in the symbol represents the sagittal suture between the PFs, while the points of the obelos depict the PF on both sides.<sup>29</sup> If the ossification period in the obelion, located in the posterior one-third of the parietal bone, is prolonged, a slit or v-shaped notch appears. This slit or v-shaped notch is occasionally referred to as the subsagittal suture of Pozzi,<sup>30</sup> fonticulus obelicus,<sup>31</sup> or pars obelica.<sup>32</sup> The formation of the sagittal suture depends on the closure of three fontanelles. The first is the anterior fontanelle between the frontal and parietal bones. The second is the posterior fontanelle between the parietal and occipital bones. The third, known as the sagittal fontanelle, contributes to the formation of unilateral or bilateral parietal foramina. This fontanelle is present in 50–80% of cases and typically closes within the first two years of life. Variations in the closure of the third fontanelle can lead to the formation of accessory parietal emissary foramina, enlarged parietal foramina, parietal fissures, or obelical bones.<sup>7</sup>

The size, presence, patency, and topography of PFs are highly variable. Identifying new anatomical features and understanding the variable topographic localization of PFs is crucial for invasive procedures involving this region.<sup>9</sup> Knowledge of PF variations is important to avoid damaging PEVs, anastomosing arteries, and neural structures that may pass through the PF during neurosurgical procedures.<sup>5</sup> This understanding helps prevent damage to these structures during invasive procedures and reduces the risk of subsequent complications.<sup>11</sup> To investigate the morphological and morphometric features of the PF, we studied 174 parietal bones. A review of the existing literature reveals that PF is often less common in white populations compared to other racial groups (Appendix). The frequency, shape, direction, diameter, DPF, DSS, LSS, DPO, and TPL observed in our study are consistent with the literature. We believe that our morphological and morphometric data may collectively aid surgeons in increasing the success rate of invasive procedures and minimizing the risk of complications.

**Limitations of the Study:** This study has several limitations. First, the sample size is relatively small. Second, since the gender of the parietal bones was unknown and it was unclear whether the bone samples belonged to the same individual, comparisons of these bone measurements in terms of gender and side could not be made. Despite these limitations, the fact that our findings are consistent with the literature strengthens the study's reliability. Furthermore, the results of the reliability analysis demonstrate that the data obtained are highly satisfactory.

## CONCLUSION

It is important to understand all the anatomical aspects of the PF, which shows anatomical variations across different races. For this purpose, we investigated the frequency, shape, direction, diameter, topographic location, and distances of the PF to certain landmarks in 174 parietal bones. This study documents more detailed anatomical findings than previous studies conducted in Türkiye. We believe that the data obtained in this study may be important in improving the success rate of invasive procedures involving the PF or its adjacent structures and in reducing or preventing complications.

**Ethics Committee Approval:** Clinical Research Ethical Committee of İstanbul Faculty of Medicine, İstanbul University granted approval for this study (date: 04.03. 2022, number: 2022/462).

**Author Contributions:** Concept – LS, İA, AES, AÖ; Design – LS, İA, AES, AÖ; Supervision – LS, İA, AES, AÖ; Materials – LS, AÖ; Data Collection and/or Processing – İA, AES; Analysis and/or Interpretation – LS, AÖ; Literature Search – LS, İA, AES, AÖ; Writing – LS, İA; Critical Reviews – LS, İA, AÖ, AES.

**Conflict of Interest:** The authors have no conflict of interest to declare.

**Informed Consent:** Not applicable.

**Use of AI for Writing Assistance:** Not declared.

**Financial Disclosure:** The authors declared that this study has received no financial support.

**Peer-review:** Externally peer-reviewed.

## REFERENCES

1. Standring S. *Gray's Anatomy: The Anatomical Basis of Clinical Practice*. 42<sup>nd</sup> ed. China: Elsevier Health Sciences; 2021.
2. Reddy AT, Hedlund GL, Percy AK. Enlarged parietal foramina: Association with cerebral venous and cortical anomalies. *Neurology* 2000; 54(5): 1175-8. [\[CrossRef\]](#)
3. Tsutsumi S, Nonaka S, Ono H, Yasumoto Y. The extracranial to intracranial anastomotic channel through the parietal foramen: Delineation with magnetic resonance imaging. *Surg Radiol Anat* 2016; 38(4): 455-9. [\[CrossRef\]](#)
4. Mortazavi MM, Tubbs RS, Riech S, Verma K, Shoja MM, Zurada A, et al. Anatomy and pathology of the cranial emissary veins: A review with surgical implications. *Neurosurgery* 2012; 70(5): 1312-8. [\[CrossRef\]](#)
5. Al-Shuaili A, Al-Ajmi E, Mogali SR, Al-Qasmi S, Al-Mufargi Y, Kariyattil R, et al. Computed-tomography evaluation of parietal foramen topography in adults: A retrospective analysis. *Surg Radiol Anat* 2024; 46(3): 263-70. [\[CrossRef\]](#)
6. de Souza Ferreira MR, Galvão APO, de Queiroz Lima PTMB, de Queiroz Lima AMB, Magalhães CP, Valença MM. The parietal foramen anatomy: Studies using dry skulls, cadaver and in vivo MRI. *Surg Radiol Anat* 2021; 43(7): 1159-68. [\[CrossRef\]](#)
7. Mann RW, Manabe J, Byrd JE. Relationship of the parietal foramen and complexity of the human sagittal suture. *Int J Morphol* 2009; 27(2): 553-64. [\[CrossRef\]](#)
8. van der Walt S, Hammer N, Prigge L. Comparison between the parietal foramina observed in samples of African and European population groups. *Int J Morphol* 2009; 41(2): 634-39. [\[CrossRef\]](#)
9. Keskil S, Gözil R, Calgüner E. Common surgical pitfalls in the skull. *Surg Neurol* 2003; 59(3): 228-31. [\[CrossRef\]](#)
10. Liu D, Yang H, Wu J, Li JH, Li YK. Anatomical observation and significance of the parietal foramen in Chinese adults. *Folia Morphol (Warsz)* 2022; 81(4): 998-1004. [\[CrossRef\]](#)
11. Shmarhalov A, Vovk O, Ikramov V, Acharya Y, Vovk O. Anatomical variations of the parietal foramen and its relations to the calvarial landmarks: A cross-sectional cadaveric study. *Wiad Lek* 2022; 75(7): 1648-52. [\[CrossRef\]](#)
12. Sağlam L, Gayretli Ö, Coşkun O, Kale A. The triangular area between the greater, lesser, and third occipital nerves and its possible clinical significance. *Surg Radiol Anat* 2024; 46(2): 185-90. [\[CrossRef\]](#)
13. Weinberg SM, Scott NM, Neiswanger K, Marazita ML. Intraobserver error associated with measurements of the hand. *Am J Hum Biol* 2005; 17(3): 368-71. [\[CrossRef\]](#)
14. Geeta A, Jamaiah H, Safiza MN, Khor GL, Kee CC, Ahmad AZ, et al. Reliability, technical error of measurements and validity of instruments for nutritional status assessment of adults in Malaysia. *Singapore Med J* 2009; 50(10): 1013-8.
15. Kemper CJ, Schwerdtfeger A. Comparing indirect methods of digit ratio (2D:4D) measurement. *Am J Hum Biol* 2009; 21(2): 188-91. [\[CrossRef\]](#)
16. Mahakkanukrauh C, Chitapanarux N, Kwangsukstith S, Navic P, Mahakkanukrauh P. The morphometric study of parietal emissary foramen related with clinical implications in thais. *Int J Morphol* 2021; 39(5): 1283-8. [\[CrossRef\]](#)
17. Yoshioka N, Rhoton AL Jr, Abe H. Scalp to meningeal arterial anastomosis in the parietal foramen. *Neurosurgery* 2006; 58(1): 123-6. [\[CrossRef\]](#)
18. Guzelad O, Ogut E, Yildirim FB. Evaluation of the parietal foramen and its surgical importance in dry skulls: A cross-sectional morphometric study. *Med Bull Haseki* 2023; 61(1): 43-51. [\[CrossRef\]](#)
19. Naidoo J, Luckrajh JS, Lazarus L. Parietal foramen: Incidence and topography. *Folia Morphol (Warsz)* 2021; 80(4): 980-4. [\[CrossRef\]](#)

20. Murlimanju BV, Saralaya VV, Somesh MS, Prabhu LV, Krishnamurthy A, Chettiar GK, et al. Morphology and topography of the parietal emissary foramina in South Indians: An anatomical study. *Anat Cell Biol* 2015; 48(4): 292-8. [\[CrossRef\]](#)
21. Gangmei G, Devi HS, Daimei T, Remei E, Tunglut J. Variations of parietal foramen in dried adult human skulls. *J Dent Med Sci* 2018; 17(5): 26-9.
22. Fating A, Pawar S. Parietal foramina in adult human skulls: An anatomical study. *Med Innov* 2020; 9(2): 46-9.
23. Wysocki J, Reymond J, Skarzyński H, Wróbel B. The size of selected human skull foramina in relation to skull capacity. *Folia Morphol (Warsz)* 2006; 65(4): 301-8.
24. Collipal E, Silva H, Quintas F, Martínez C, Sol M. Morphometry study of the parietal foramen. *Int J Morphol* 2009; 27(2): 481-4. [\[CrossRef\]](#)
25. Shantharam V, Manjunath KY. Anatomical study of parietal emissary foramina in human skulls. *Int J Anat Radiol Surg* 2018; 7(1): 11-4.
26. Halagatti M, Sagar S. An anatomical study of parietal emissary foramina in dry adult human skulls. *Int J Anat Radiol Surg* 2018; 7(2): A020-2.
27. Hoheisel WF. An anomalous Indian occiput. *Anat Rec* 1930; 45(2): 129-35. [\[CrossRef\]](#)
28. Steele DG, Bramblett CA. The anatomy and biology of the human skeleton. USA: Texas A&M University Press; 1988.
29. Jamieson EB. Dixon's manual of human osteology. 2<sup>nd</sup> ed. London: Humphrey Milford; 1937.
30. Breathnach AS. Frazer's anatomy of the human skeleton. 6<sup>th</sup> ed. London: J&A Churchill Ltd.; 1965.
31. Pernkopf E. Atlas of topographical and applied human anatomy. Philadelphia: WB Saunders; 1963.
32. Scheuer L, Black SM. The juvenile skeleton. Amsterdam: Elsevier Academic Press; 2004. [\[CrossRef\]](#)